

VIP **Batteries** Very Important Paper
How to cite: *Angew. Chem. Int. Ed.* **2023**, *62*, e202301253

International Edition: doi.org/10.1002/anie.202301253

German Edition: doi.org/10.1002/ange.202301253

Entropic Contributions to Sodium Solvation and Solvent Stabilization upon Electrochemical Sodium Deposition from Diglyme and Propylene Carbonate Electrolytes

Franziska Karcher, Matthias Uhl, Tanja Geng, Timo Jacob, and Rolf Schuster*

Abstract: The formation of an appropriate solid electrolyte interphase (SEI) at the anode of a sodium battery is crucially dependent on the electrochemical stability of solvent and electrolyte at the redox potential of Na/Na⁺ in the respective system. In order to determine entropic contributions to the relative stability of the electrolyte solution, we measure the reaction entropy of Na metal deposition for diglyme (DG) and propylene carbonate (PC) based electrolyte solutions by electrochemical microcalorimetry at single electrodes. We found a large positive reaction entropy for Na⁺ deposition in DG of $\Delta_{\text{R}}S(\text{DG}) \approx 234 \text{ J mol}^{-1} \text{ K}^{-1}$ (c.f.: $\Delta_{\text{R}}S(\text{PC}) \approx 83 \text{ J mol}^{-1} \text{ K}^{-1}$), which signals substantial entropic destabilization of Na⁺ in DG by about 0.73 eV, thus increasing the stability of solvent and electrolyte relative to Na⁺ reduction. We attribute this strong entropic destabilization to a highly negative solvation entropy of Na⁺, due to the low dielectric constant and high freezing entropy of DG.

Introduction

Triggered by the high demand for effective energy storage and the natural abundance of sodium, Na batteries may become an attractive alternative to Li-ion batteries. The use of Na metal anodes is, however, usually hampered by low

reversibility of the Na plating/stripping processes as well as by pronounced dendrite formation, due to the high reactivity of metallic Na with the solvent.^[1] Recently, Seh et al. demonstrated that these obstacles can be circumvented by the use of glyme-based (mono-, di-, and tetraglyme) NaPF₆ electrolyte solutions.^[2] These authors observed highly reversible, non-dendritic Na-plating pointing to the formation of a stable, compact solid electrolyte interphase (SEI). Usually the SEI consists of a layer of organic and inorganic electrolyte and solvent decomposition products, which effectively prevents ongoing decomposition, while sustaining Na deposition/dissolution by its ionic conductivity.^[2,3] In their seminal study, Seh et al. compared the composition of the SEI in glyme-based electrolytes with that of carbonate solutions and attributed the excellent properties of the SEI to its high inorganic content, which originates from the preferential decomposition of the electrolyte compared to the reduction of the glyme-based solvents.^[2] In contrast, in carbonate containing electrolytes, the SEI exhibits a higher content of organic products. This was attributed to a rather negative reduction potential of ether solvents, compared to the carbonates, rendering ether solvents thermodynamically stable at the redox potential of the Na metal electrode. This relative stability of the solvent referred to the Na/Na⁺ redox potential can be ascribed either to a more stable organic solvent molecule, which would shift the reduction potential of the solvent negatively, or conversely, it may be due to a destabilized Na⁺-solvent complex in solution, which would shift the redox potential of Na/Na⁺ positively.^[4] In the latter case, the solvation properties of Na⁺ in the glyme-based solvents are of crucial importance for the proper formation of the SEI.^[4,5]

In the present work, we quantitatively study the entropic contributions to the thermodynamic stability of Na⁺ complexes in 1 M NaPF₆/diglyme solution. We approach this quantity by determining the entropy of reaction for the sodium deposition in diglyme solutions by half-cell microcalorimetry (HCMC).^[6,7] For this purpose, we measure the heat reversibly exchanged at a single Na metal electrode, which is directly correlated to the reaction entropy of the Na⁺ reduction process.^[8,9] The entropy values obtained in diglyme solutions are compared with the reaction entropy in a carbonate based electrolyte (1 M NaClO₄/propylene carbonate (PC)), which is a well-established electrolyte for sodium ion batteries.^[10] Within a simple model by Marcus,^[11] we discuss the contributions to the reaction entropy of sodium deposition, calculate coordination numbers of the

[*] F. Karcher, R. Schuster
 Institute of Physical Chemistry, Karlsruhe Institute of Technology
 (Germany)
 E-mail: rolf.schuster@kit.edu

M. Uhl, T. Geng, T. Jacob
 Institute of Electrochemistry, Ulm University (Germany)

T. Jacob
 Helmholtz-Institute-Ulm (HIU) Electrochemical Energy Storage
 Ulm (Germany)
 and
 Karlsruhe Institute of Technology (KIT)
 Karlsruhe (Germany)

© 2023 The Authors. Angewandte Chemie International Edition published by Wiley-VCH GmbH. This is an open access article under the terms of the Creative Commons Attribution Non-Commercial NoDerivs License, which permits use and distribution in any medium, provided the original work is properly cited, the use is non-commercial and no modifications or adaptations are made.

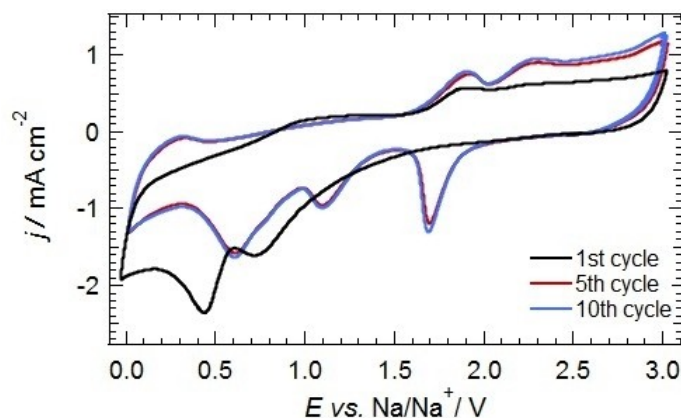


Figure 1. CV of a pristine Cu-foil in 1 M NaPF₆ in diglyme with a scan rate of 50 mVs⁻¹. The different cathodic and anodic peaks become stable after about 5 cycles.

ions and derive implications on the influence of solvent entropy on the half-cell potential of the Na metal electrode and solvent stability.

Results and Discussion

Pretreatment of the Cu current collector and preparation of a Na layer

Before the half-cell microcalorimetric measurements, we performed a pretreatment of the pristine Cu foil by cyclic voltammetry (for experimental details see Supporting Information). Figure 1 shows a typical cyclic voltammogram (CV) of the Cu surface in 1 M NaPF₆/diglyme for an electrochemical window from 3 V to 0 V recorded with 50 mVs⁻¹. While in the first cathodic scan only two broad peaks at 0.8 V and 0.4 V are visible, the CV quickly stabilizes showing essentially three pronounced cathodic peaks at about 0.6 V, 1.2 V and 1.7 V, an anodic one at 1.9 V, and a wide anodic wave between about 2.1 V and 3 V. Below about 1 V, the CVs exhibit a considerable negative background current, which slightly decreases for higher cycle numbers. In accordance with Wang et al.,^[12] we ascribe the negative background current to the irreversible decomposition of electrolyte or solvent and SEI formation. This is supported by EQCM measurements performed on Cu-coated quartz crystals, where potential and frequency variation were recorded during application of a reduction current of -1 mA cm^{-2} . In Figure 2, the chronopotentiometric curve (a) starting at 2.2 V and the frequency variation (b) are shown. Previous to the EQCM experiment, the Cu surface was cycled between 3 V and 0 V, so that the surface condition corresponds to that of the higher cycle numbers in the CV of Figure 1. As can be clearly seen in Figure 2 (b), after a few seconds, when the potential drops below about 1 V, the (negative) slope of the frequency curve increases, signaling strong deposition of material onto the electrode. The related mass change per moles of electrons was determined from the Sauerbrey equation^[13] analogously to

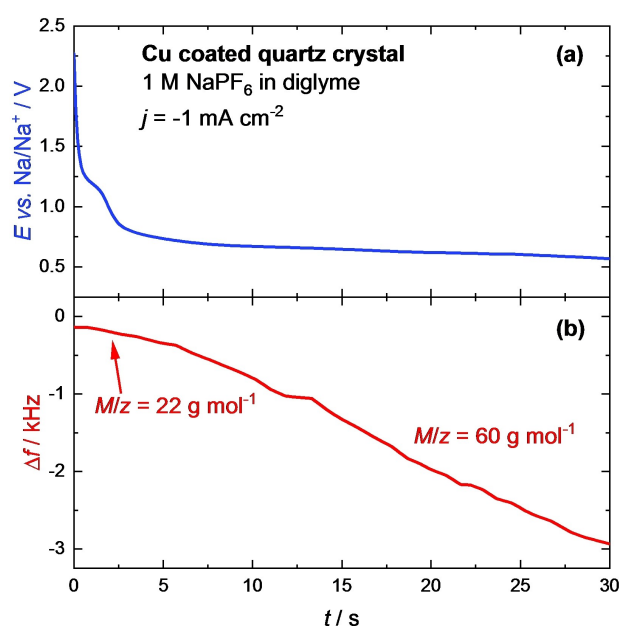


Figure 2. Chronopotentiometric EQCM measurement of a copper-coated quartz crystal in 1 M NaPF₆ in diglyme upon reduction with a current of -1 mA cm^{-2} , (a) potential vs. time, (b) change of resonance frequency vs. time. The numbers in (b) indicate the mass per moles of electrons of the deposited species according to the Sauerbrey equation.

the procedure of Geng and co-workers,^[14] resulting in about 60 g mol^{-1} . This is well above the expected value for Na deposition (23 g mol^{-1}) and points to the deposition of a reaction product with high molecular weight, which indicates the ongoing formation of the SEI. Seh et al. showed by XPS that the SEI in 1 M NaPF₆ in diglyme mostly consists of Na₂O (from the reaction of Na with minor O₂ contaminations) and NaF (due to salt reduction) accompanied by a smaller amount of sodium alkoxides as reduction products of diglyme. They supposed that the NaPF₆ solute has a more positive reduction potential than diglyme and is therefore preferably reduced.^[2] This assumption also fits with the results of Westman et al.^[4] They calculated the reduction

potentials of different glyme species in the electrolyte, all of which were below 0 V vs. Na/Na⁺.

After the first cycles in the CV of Figure 1, anodic and cathodic peaks appear above 1 V, which may at least partly result from conversion reactions of the Cu surface or its natural oxides. For example, Klein et al. discussed the thermodynamic properties of different conversion electrodes and compared them with results of XRD and electrochemical measurements.^[15] They concluded that the conversion of Na and CuO to Cu and Na₂O proceeds via Cu₂O as an intermediate phase (at 1.36 V vs. Na/Na⁺). Later they corroborated their investigation of the reaction mechanism and surface film formation on sputtered CuO thin films with cyclic voltammetry, scanning electron microscopy (SEM), and X-ray photoelectron spectroscopy (XPS).^[16] They found that the conversion reaction between CuO and Na is only partly reversible, i.e., Cu is not completely reoxidized to CuO after the first discharging process. In the following cycles, only the conversion between Cu₂O and Cu remains reversible with a theoretical redox potential of 1.18 V (vs. Na/Na⁺). This fits perfectly to the cathodic peak, which becomes stabilized at 1.2 V after the first few cycles of the CV in Figure 1. The conversion of Na and copper oxide is corroborated by our EQCM measurements, where the mass change per mole of electrons at potentials around 1.2 V amounted to 22 g mol⁻¹ (see Figure 2 during and shortly after the small potential plateau at 1.2 V vs. Na/Na⁺). This corresponds within experimental errors to the molar mass of sodium (23 g mol⁻¹), indicating the incorporation of Na⁺ into copper oxides on the electrode surface. In contrast to the peak at 1.2 V, we do not detect any mass changes for the cathodic peak at 1.7 V. Note that this peak appears only after the surface was polarized beyond ca. 2.2 V during the positive potential scan. This rules out reduction of impurities such as water in the bulk of the electrolyte but rather points to a faradaic reaction at the (oxidized) Cu surface.

It should be noted that the pretreatment of the Cu foil has strong impact on the stability of the deposited Na layer and on the following HCMC measurements. In particular, if we cathodically extended the electrochemical window to -0.3 V during the first CV cycle, we noticed spikes and irregular jumps in the cathodic current for potentials < 0 V. Similar effects were reported, e.g., by Sun et al.^[17] They compared the plating and stripping behavior of Na from NaPF₆ in diglyme on planar and 3D porous Cu current collectors and detected strong fluctuations in the voltage profile for Na plating/stripping on the planar Cu surface. They ascribed this behavior to the fracture of Na dendrites and an ongoing SEI reformation. As a consequence of a negative potential scan to -0.3 V in the first CV cycle, the deposition of a stable and active Na surface was impeded also in subsequent scans, which was recognized by an unstable open circuit potential (OCP). In addition to the current fluctuations in the CV for potentials negative of 0 V, we also detected random spikes in the temperature signal of the HCMC. As mentioned in the experimental section, we use a pyroelectric LiTaO₃ sensor for temperature detection, which exhibits also piezoelectric response. We thus attribute these spikes on the temperature signal to charge pulses of

the piezoelectric sensor, originating from the release of mechanical strain in the SEI-covered Na surface, e.g., by the formation of cracks.

In NaClO₄/PC solutions, we observed neither fluctuations nor spikes on the cell potential or on the sensor signal, indicating that the latter system is less sensitive to the pretreatment of the electrode. However, to obtain reproducible Na surfaces for the HCMC experiments in both, PC and diglyme based electrolytes, prior to Na deposition, we always cycled the Cu current collector 10 times within a potential window between 3 and 0 V, before we electrochemically plated Na with a current density of -1.25 mA cm⁻² for about 20 minutes. By the described procedure, we received a thick, active and stable Na surface, indicated by an OCP around 0 V, with a thickness of about 3.7 μm, assuming a homogeneous film (see Supporting Information).

Determination of the entropy of Na deposition in diglyme and PC solutions

Figure 3 shows typical potential, current, temperature, and heat transients of HCMC experiments for Na deposition (a) and dissolution (b) on a Na layer in 1 M NaPF₆ in diglyme by 10 ms potential pulses with -100 mV and +100 mV amplitudes. The experiments started by switching the cell to OCP about 100 ms before recording the transients in Figure 3. Thus, by avoiding any external current flow, the adjustment of the Na/Na⁺ equilibrium potential was allowed prior to the potential pulse. For the application of the potential pulse, the cell was returned to potential control at *t* = 10 ms and a potential pulse was applied. At the end of the pulse, at *t* = 20 ms the cell was switched back to OCP, avoiding again any external current flow after the pulse. The corresponding current (black) parallels the potential transient. It stays constant during the pulse, indicating that no concentration gradient has built up and that there were no transport limitations during the 10 ms reaction. For the experiments in Figure 3, the charge that flowed within the short pulse corresponds to deposition of about 9% of a complete monolayer, referenced to the topmost layer of a densely packed Cu surface. During the negative potential pulse (Figure 3 (a)), the temperature of the electrode (orange) linearly drops and reaches its minimum shortly after the end of the potential pulse. After the pulse, when the external current flow ceased, the temperature slowly relaxes towards its starting value by heat uptake from the surrounding. As mentioned in the Supporting Information, by deconvolution with the thermal response function of the cell, the evolved total heat can be determined as a function of time. The resulting heat transient (red) is shown in the lowest trace of Figure 3 (a). After *t* = 10 ms, with the beginning of the potential pulse, the total evolved heat linearly decreases signaling a constant negative heat flux, i.e., cooling during the pulse. After the potential pulse, a small, continuing, negative heat flux is observed, which effectively ceases at about 60 ms. The heat evolved after the pulse amounts to only about 10% of the heat evolved during

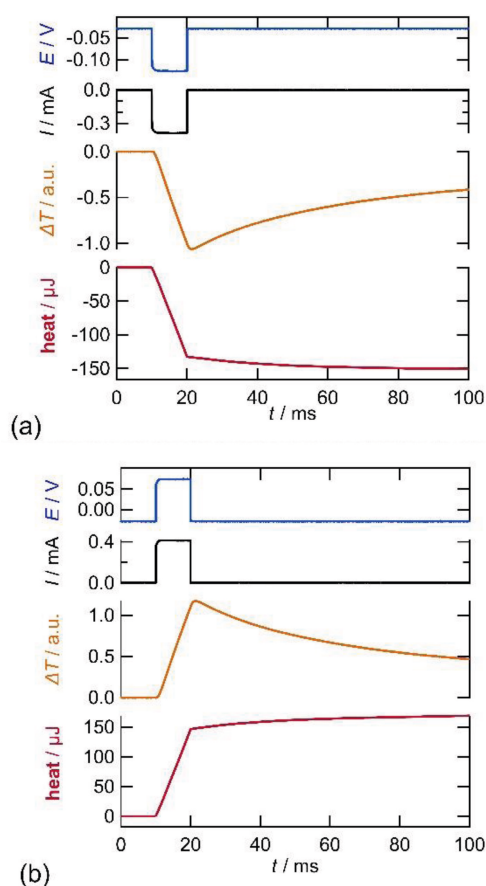


Figure 3. Potential E , current I , temperature ΔT and heat transients resulting from 10 ms potential pulses ($|\eta| = 100$ mV) with negative (a) and positive (b) polarity on a Na plated Cu foil in 1 M NaPF₆ in diglyme. The pulses were applied at the equilibrium potential of about 0 V. After the pulses, at $t = 20$ ms, the cell was switched to open circuit conditions. The electrode cools down during Na-deposition and heats up during Na-dissolution.

current flow. It follows from the definition of the entropy, $dS = \delta q_{\text{rev}}/T$, that for the quantitative determination of the entropy change of the overall electrochemically driven sodium deposition process the complete reversibly exchanged heat q_{rev} has to be determined. Therefore, in the following, we evaluate the heat at $t = 100$ ms to securely measure the total heat evolved by the electrochemically driven processes. We attribute the heat flux after the 10 ms current pulse to charge-neutral equilibration processes, following the external current flow. Similar effects were observed for Ag bulk deposition, where the delayed heat flux could be quantitatively explained by ongoing Ag deposition due to discharging of the double layer after the current pulse.^[7] In the present case, also equilibration processes following the transport of Na⁺ through the SEI might contribute.

Data for sodium dissolution with 100 mV positive potential pulses is shown in Figure 3 (b). With positive potential pulses, the electrode is warming up and all three, current, temperature, and heat transients, possess the same shape and reach about the same absolute values as in Figure 3 (a), albeit with opposite sign. This already signals that the Na deposition/dissolution process is highly reversible and that the system stays close to thermodynamic equilibrium during the short disturbance by the potential pulse. For a quantitative evaluation of the reversibly exchanged heat, we conducted several potential pulse experiments with different amplitudes, i.e., overpotentials, with positive and negative polarities ($|\eta| = 0.05$ – 0.2 V). The measured heat (at $t = 100$ ms) was then normalized to the moles of elementary charges, which flowed through the cell circuit during the reaction, to obtain the molar heat q_{mol} . For the determination of the reversible part of the exchanged heat at the Na electrode (q_{rev}), the so called Peltier heat Π , we plotted the different values of q_{mol} versus the respective overpotential and interpolated to $\eta = 0$ V (Figure 4) (see, e.g., ref. [7] for further details). By this procedure, from the data in Figure 4, we obtained a value of 75 kJ mol^{-1} for the reversibly exchanged heat of sodium deposition in 1 M

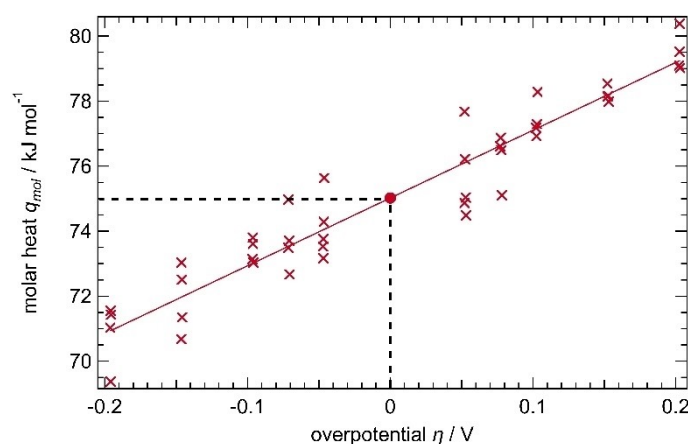


Figure 4. Molar heat for Na deposition obtained by potential pulses with varying overpotential and polarity ($|\eta| = 0.05$ V to 0.2 V) on a Na-plated Cu foil in 1 M NaPF₆ in diglyme. The value of the molar heat interpolated towards $\eta = 0$ V corresponds to the reversibly exchanged heat during the Na deposition/dissolution reaction.

NaPF₆ in diglyme on a Na surface. The average of in total 18 experiments on freshly prepared Na surfaces amounts to 75.2 kJ mol⁻¹ ± 2.9 kJ mol⁻¹, where a positive Peltier heat means cooling of the electrode upon the cathodic process direction. The corresponding entropy change ΔS at the single electrode is given by $\Delta S = \frac{q_{rev}}{T}$ and amounts to 252 J mol⁻¹ K⁻¹.

Analogous experiments were conducted for Na deposition and dissolution in 1 M NaClO₄ in PC solutions. Corresponding potential, current, temperature, and heat transients as well as plots of the molar heat vs. overpotential can be found in the Supporting Information (Figures S1 and S2). Those experiments yielded a Peltier heat of 25.0 kJ mol⁻¹ ± 2.7 kJ mol⁻¹, corresponding to an entropy change of about 84 J mol⁻¹ K⁻¹ for Na deposition in 1 M NaClO₄ in PC.

It should be noted at this point that, since we measure the reversibly exchanged heat of a half-cell, the determined Peltier heat and thus also the entropy change ΔS contain contributions from ion transport in solution.^[9] These contributions to the reversibly exchanged heat were estimated using an approximation by Agar (see Supporting Information, section 3, Tables S1 and S2).^[9] For the carbonate system, transport contributes less than 1 kJ mol⁻¹ to the reversible molar heat, which is below the expected experimental error. In the diglyme system, the contribution of transport is slightly higher ($T\Delta_T S \approx -5.2$ kJ mol⁻¹), which results from the smaller permittivity of the diglyme solvent compared to PC. After correcting for the heat of transport, using equation S4 in the Supporting Information, we receive a reaction entropy of the Na deposition process in the NaPF₆/diglyme electrolyte of $\Delta_R S \approx 234$ J mol⁻¹ K⁻¹ ($T\Delta_T S \approx 70$ kJ mol⁻¹). For Na deposition from PC, we obtained $\Delta_R S \approx 83$ J mol⁻¹ K⁻¹ ($T \cdot \Delta_R S \approx 25$ kJ mol⁻¹).

Estimation of the solvation number of Na⁺ in diglyme and PC solutions

In both solvents, the entropy change during the Na deposition process at the Na electrode is strongly positive. Such a positive entropy change is not expected for pure immobilization of Na⁺ ions on the electrode surface upon deposition, but can be explained considering the influence of the solvent. In the solution, diglyme or PC molecules are fixed in the solvation shell of the Na⁺ ions and are released during the deposition process. The corresponding gain of entropy through the release of solvent molecules obviously outweighs the entropy loss from the immobilization of the Na⁺ ions, leading to a positive entropy change for the overall process. In previous publications,^[18,19] we employed a simple model, proposed by Marcus,^[11] to estimate the entropy change due to immobilization of solvent molecules in the first solvation shell for the Li⁺ solvation in 1 M LiPF₆ in EC/DMC and to estimate the solvation number of the Li⁺ ions. In the following, we employ this model to the currently studied systems. In brief, the reaction entropy can be split in three contributions:

$$\Delta_R S = \Delta_{Na} S - \Delta_{Born} S - \Delta_{immob} S \quad (1)$$

The entropic contribution of the electron in the metal electrode is small (ca. 0.48 J mol⁻¹ K⁻¹^[20]) and is therefore neglected in this approximation. $\Delta_{Na} S$ is the entropy change due to the immobilization of Na⁺ ions on the surface of the electrode. It can be estimated from the entropy of freezing of sodium (7 J mol⁻¹ K⁻¹ at $T = 368$ K),^[21] which has to be corrected for room temperature and the concentration of a 1 M Na⁺ solution. Following the procedure described in the Supporting Information, we estimated $\Delta_{Na} S \approx -37.5$ J mol⁻¹ K⁻¹. The second contribution, the Born entropy $\Delta_{Born} S$, reflects the impact of solvent molecules in the 2nd and higher solvation shells on $\Delta_R S$ upon desolvation of the Na⁺ ions. By Born's approximation, which is based on the charging of an ion in a homogeneous dielectric, this contribution can be calculated from the dielectric constant, its temperature derivative, and the radius of the Na⁺-solvent complex including its first solvation shell. The radius of the first solvation shell of the diglyme complex was found to be 0.425 nm by DFT calculations.^[22] For the radius of the Na⁺/PC complex, we employed 0.636 nm,^[11] obtained by summation of the Pauling radius of Na⁺ and the hard-sphere diameter of PC. Together with dielectric constants of 7.36 and 65 for diglyme^[23] and PC^[24] and temperature derivatives of -0.027 K⁻¹^[23] and -0.23 K⁻¹,^[24] we obtained $\Delta_{Born} S \approx -81$ J mol⁻¹ K⁻¹ for diglyme and -6 J mol⁻¹ K⁻¹ for PC (see equation S7). Notably, the Born entropy in the diglyme solution is considerably negative, which originates from the small dielectric constant of diglyme and which signals the weak screening of the ion charge by its 1st solvation shell. The last term in equation (1), $\Delta_{immob} S$, represents the entropy loss from fixation of solvent molecules in the first solvation shell of Na⁺ and is the only unknown quantity in this equation. Analogously to $\Delta_{Born} S$, this entropy contribution is set free upon desolvation of the ion. With the experimentally determined reaction entropy, we can now solve equation (1) for $\Delta_{immob} S$ and yield $\Delta_{immob} S \approx -191$ J mol⁻¹ K⁻¹ for Na⁺ in diglyme and $\Delta_{immob} S \approx -119$ J mol⁻¹ K⁻¹ in PC. The solvent immobilization entropies may be compared with the entropies of freezing of the respective solvents.^[11] The latter ones reflect a very similar process to the formation of the first solvation shell, namely the transfer of solvent molecules from the mobile liquid phase to a solid phase, where solvent movement is effectively suppressed. From the entropies of freezing of -85 J mol⁻¹ K⁻¹ at $T = 209.1$ K for diglyme^[25] and -37 J mol⁻¹ K⁻¹ at $T = 224.9$ K for PC^[26] and the respective heat capacities, we calculated the corresponding values for the (hypothetical) entropies of freezing at room temperature (-115 J mol⁻¹ K⁻¹ and -51 J mol⁻¹ K⁻¹), following the approximation described in the Supporting Information (see equation S8 and Table S3). Note that the entropy of freezing refers to moles of solvent molecules, while the entropy of immobilization is referenced to moles of Na⁺ ions. Thus, the ratio of the two quantities provides an estimate of the number of solvent molecules bound in the first solvation shell of a Na⁺ ion, which corresponds to the

coordination number of Na^+ in the respective solvent. We found values of 1.7 for Na^+ /diglyme and 2.3 for Na^+ /PC.

The coordination number for Na^+ in diglyme compares well with those proposed by other investigations. For example, Tanwar et al.^[27] found a coordination number of 2 of Na^+ in diglyme by DFT calculations. Jensen et al. investigated the structure of solvated Na^+ in 1 M NaPF_6 in diglyme by neutron diffraction^[28] and showed that the main conformation is a $\text{Na}^+(\text{diglyme})_2$ complex with a distorted octahedral structure. In addition, a smaller fraction of the complexes (18 %) also formed contact ion pairs. It should be mentioned that in the simple model applied above, we did not consider formation of ion pairs and their influence on the solvation entropy.

For Na^+ in PC, we found a coordination number which is slightly lower than common values known from literature. For example, Kamath et al. investigated the interaction of Na^+ with several cyclic and linear carbonate solvents by classical molecular dynamics. Their calculations suggest the coordination of 3 to 3.5 PC molecules per Na^+ ion via the carbonyl oxygen.^[29] Liu et al. compared the stepwise Na^+ solvation reaction in different carbonate and ether solvents based on density functional theory. By calculating the Gibbs free energies, they obtained a coordination number of 4 for Na^+ in PC.^[30] The deviation of our results may indicate that PC molecules are relatively loosely bound in the 1st coordination shell of the Na^+ ion and that therefore the freezing entropy of PC overestimates the contribution to $\Delta_{\text{immob}}S$ upon the fixation of the PC molecules in the solvation shell. It should be noted that there exist studies on the entropy of solvation of Na^+ in PC in literature. Marcus, for example, used experimental values of the standard molar entropy of hydration and the entropy change upon the transfer of Na^+ from water into PC to calculate the standard molar entropy of solvation $\Delta_{\text{sol}}S^0$.^[11] Converted to absolute scale, his calculations lead to $\Delta_{\text{sol}}S^0 \approx -186 \text{ J mol}^{-1} \text{ K}^{-1}$, which describes the entropy change upon transfer of Na^+ from a hypothetical gas in its standard state into the solvent. In our work, immobilization and Born entropies refer to the entropy changes in the first and higher coordination shells upon solvation of Na^+ from an ideal 1 M solution. Thus, by taking the sum of immobilization and Born entropies and correcting for the change of the standard state from a gas phase at standard conditions to a 1 M ideal solution, we can directly calculate the standard entropy of solvation from our data. The entropy difference between the standard states was given by Marcus and amounts to $-26.7 \text{ J mol}^{-1} \text{ K}^{-1}$.^[11] From our data, we end up with a standard entropy of solvation of Na^+ in PC of $\Delta_{\text{sol}}S^0 \approx -148 \text{ J mol}^{-1} \text{ K}^{-1}$, which compares well with the results of Marcus,^[11] considering the involved approximations in both, Marcus' and our calculations. Shakourian-Fard et al. used molecular dynamic simulations to calculate the enthalpy, free enthalpy, and entropy of solvation of Na^+ in carbonate-based solvents.^[31] They found $\Delta_{\text{sol}}H \approx -426 \text{ kJ mol}^{-1}$ and $\Delta_{\text{sol}}G \approx -290 \text{ kJ mol}^{-1}$. This corresponds to a solvation entropy of $\Delta_{\text{sol}}S \approx -450 \text{ J mol}^{-1} \text{ K}^{-1}$ for the transfer of a hypothetical Na^+ ion in the standard state in the gas phase into the solvent. Thus, the theoretical solvation entropy seems

unexpectedly large and is neither compatible with our heat measurements nor with the results of Marcus. Note, however, that this deviation may also be caused by the chosen standard state of Na^+ in the calculations, which is not explicitly stated in ref. [31]. Another theoretical study by Kamath et al. calculated $\Delta_{\text{sol}}G$ for Na^+ in PC by the adaptive biasing force method.^[29] They received a value of around -52 kJ mol^{-1} , which considerably differs from the value given in ref. [31].

Entropic contributions to the half-cell potential for sodium reduction and to the stability of the solvent

By HCMC, we directly determined the reaction entropy of the half-cell reaction, $\text{Na}^+_{\text{sol}} + e^- \rightarrow \text{Na}_m$ and thus the entropic contribution $-T \Delta_R S$ to the free enthalpy $\Delta_R G$ of this reaction. The latter is given by $\Delta_R G = \Delta_R H - T \Delta_R S$, where $\Delta_R H$ is the reaction enthalpy. $\Delta_R G$ is directly correlated with the Galvani potential difference at the interface ϕ_{galv} via $\Delta_R G = -F n_e \phi_{\text{galv}}$, where F is the Faradaic constant and n_e gives the number of electrons involved in the reduction reaction. For Na^+ deposition in diglyme solutions, the entropic part of the free enthalpy of the half-cell reaction amounts to -70 kJ mol^{-1} (corrected for the heat of transport). Hence, the entropic contribution to the free enthalpy of reaction strongly destabilizes the Na^+ -diglyme complex and shifts the redox potential for Na^+ reduction positively by about 0.73 V, referenced to its value expected from purely enthalpic contributions to $\Delta_R G$. For PC, the entropic potential shift amounts to only 0.26 V. In other words, the entropy gain during desolvation of Na^+ is considerably higher in diglyme than in PC, which, following the above discussion, has two origins: i) the highly negative entropy of freezing of diglyme and ii) the highly negative Born entropy in diglyme, which reflects the weak screening of the ion charge by its first solvation shell in the weakly polarizable diglyme solvent. The weak screening leads to strong immobilization of solvent molecules also in higher solvation shells. Unfortunately, a direct comparison between the Galvani potentials for Na^+ reduction in diglyme and PC is not possible, since we found no quantitative data on the solvation enthalpy of Na^+ in diglyme.

Similar to its impact on the Na^+ reduction potential, the entropy of the solvent will also influence the reduction potential of the solvent molecules. Higher entropy of the solvent molecules in the liquid state, signaled by a highly negative entropy of freezing, will stabilize the solvent and will therefore shift the reduction potential for solvent decomposition to more negative values. A quantitative estimate would require the detailed consideration of the reaction products, however, if those were essentially solid products, the indicated trend will prevail. Thus, a high solvent entropy, reflected by a highly negative entropy of freezing, will basically have two effects. It will shift the reduction potential of Na^+ positively and that of the solvent molecules negatively. In sum, both potential shifts reduce the tendency of solvent decomposition upon Na metal deposition. A low dielectric constant of the solvent will

further promote this trend. This is in line with the results of Seh et al. in their comparative study on SEI formation and Na deposition from glyme- and carbonate-based electrolytes.^[2] In glyme-based electrolytes (with highly negative entropy of freezing and low dielectric constant), the inner part of the SEI predominately contained inorganic compounds, which stemmed from salt decomposition rather than from the reduction of the solvent. On the other hand, the SEI in carbonate-based electrolytes contained mainly organic constituents, signaling effective solvent reduction at the Na⁺ reduction potential.

Conclusion

By measuring the reversibly exchanged heat upon Na deposition from diglyme and PC based solutions, we found positive reaction entropies for Na deposition of 234 J mol⁻¹ K⁻¹ in diglyme and 83 J mol⁻¹ K⁻¹ in PC, signaling strong entropic contributions from desolvation of the ions upon metal deposition. We attribute the unexpectedly high entropy changes in diglyme solutions to the low dielectric constant of diglyme and its high entropy of freezing. As a direct consequence, such rather strong positive entropy changes will lead to considerable cooling of the metal electrode upon battery charging.^[19] It is noteworthy, that at the opposite electrode, where in a conventional sodium battery Na⁺ ions will enter the solution from the cathode material, an opposite entropic effect of about the same order of magnitude is expected from liberation and solvation of alkali ions. The observed high entropy changes considerably contribute to the free enthalpy of the electrode reactions and thus appreciably influence the (half-cell) equilibrium potentials of both, the Na deposition process and the decomposition of the electrolyte solution. We are aware that our arguments remain rather qualitative as long as the enthalpic contributions to the free enthalpy of reaction are not considered. However, we think that our data show that entropic contributions may lead to considerable shifts of the redox potentials of the associated reactions, well of the order of 0.5 eV to 1 eV.

Acknowledgements

We thank Julian Becherer, Stefan Mück, Reiner Mönig, Krishnaveni Palanisamy and Christine Kranz for providing the electrolyte solutions. This work contributes to the research performed at CELEST (Center for Electrochemical Energy Storage Ulm-Karlsruhe) and was funded by the German Research Foundation (DFG) under Project ID 390874152 (POLiS Cluster of Excellence). Open Access funding enabled and organized by Projekt DEAL.

Conflict of Interest

The authors declare no conflict of interest.

Data Availability Statement

The data that support the findings of this study are available from the corresponding author upon reasonable request.

Keywords: Electrochemical Microcalorimetry · Entropic Stabilization · Sodium Metal Deposition · Solid Electrolyte Interphase · Solvation Entropy

- [1] a) R. Cao, K. Mishra, X. Li, J. Qian, M. H. Engelhard, M. E. Bowden, K. S. Han, K. T. Mueller, W. A. Henderson, J.-G. Zhang, *Nano Energy* **2016**, *30*, 825; b) L. Medenbach, C. L. Bender, R. Haas, B. Mogwitz, C. Pompe, P. Adelhelm, D. Schröder, J. Janek, *Energy Technol.* **2017**, *5*, 2265.
- [2] Z. W. Seh, J. Sun, Y. Sun, Y. Cui, *ACS Cent. Sci.* **2015**, *1*, 449.
- [3] J. Song, B. Xiao, Y. Lin, K. Xu, X. Li, *Adv. Energy Mater.* **2018**, *8*, 1703082.
- [4] K. Westman, R. Dugas, P. Jankowski, W. Wiczorek, G. Gachot, M. Morcrette, E. Irisarri, A. Ponrouch, M. R. Palacín, J.-M. Tarascon, et al., *ACS Appl. Energy Mater.* **2018**, *1*, 2671.
- [5] a) Y. Li, F. Wu, Y. Li, M. Liu, X. Feng, Y. Bai, C. Wu, *Chem. Soc. Rev.* **2022**, *51*, 4484; b) S. K. Vineeth, C. B. Soni, Y. Sun, V. Kumar, Z. W. Seh, *Trends Chem.* **2022**, *4*, 48.
- [6] a) R. Schuster, *Curr. Opin. Electrochem.* **2017**, *1*, 88; b) J. Asenbauer, A.-L. Wirsching, M. Lang, S. Indris, T. Eisenmann, A. Mullaliu, A. Birozzi, A. Hoeffling, D. Geiger, U. Kaiser, et al., *Adv. Sustainable Syst.* **2022**, *6*, 2200102.
- [7] K. R. Bickel, K. D. Etzel, V. Halka, R. Schuster, *Electrochim. Acta* **2013**, *112*, 801.
- [8] T. Ozeki, N. Ogawa, K. Aikawa, I. Watanabe, S. Ikeda, *J. Electroanal. Chem. Interfacial Electrochem.* **1983**, *145*, 53.
- [9] J. N. Agar in *Advances in Electrochemistry and Electrochemical Engineering* (Ed.: P. Delehay), Interscience Publisher, London, **1963**, pp. 31–121.
- [10] A. Hofmann, Z. Wang, S. P. Bautista, M. Weil, F. Müller, R. Löwe, L. Schneider, I. U. Mohsin, T. Hanemann, *Electrochim. Acta* **2022**, *403*, 139670.
- [11] Y. Marcus, *J. Solution Chem.* **1986**, *15*, 291.
- [12] L. Wang, K. Zhang, Z. Hu, *Nano Res.* **2014**, *7*, 199.
- [13] G. Sauerbrey, *Z. Phys.* **1959**, *155*, 206.
- [14] T. Geng, B. W. Schick, M. Uhl, A. J. C. Kuehne, L. A. Kibler, M. U. Cebelin, T. Jacob, *ChemElectroChem* **2022**, *9*, e202101263.
- [15] F. Klein, B. Jache, A. Bhide, P. Adelhelm, *Phys. Chem. Chem. Phys.* **2013**, *15*, 15876.
- [16] F. Klein, R. Pinedo, P. Hering, A. Polity, J. Janek, P. Adelhelm, *J. Phys. Chem. C* **2016**, *120*, 1400.
- [17] J. Sun, C. Guo, Y. Cai, J. Li, X. Sun, W. Shi, S. Ai, C. Chen, F. Jiang, *Electrochim. Acta* **2019**, *309*, 18.
- [18] a) M. J. Schmid, K. R. Bickel, P. Novák, R. Schuster, *Angew. Chem. Int. Ed.* **2013**, *52*, 13233; b) M. Schmid, *Dissertation*, Karlsruher Institut für Technologie, Karlsruhe, **2014**.
- [19] M. J. Schmid, K. R. Bickel, P. Novák, R. Schuster, *Angew. Chem.* **2013**, *125*, 13475.
- [20] A. L. Rockwood, *Thermochim. Acta* **2009**, *490*, 82.
- [21] D. R. Lide, *CRC Handbook of chemistry and physics*, CRC Press, Boston, **2003**.
- [22] M. Goktas, C. Bolli, E. J. Berg, P. Novák, K. Pollok, F. Langenhorst, M. v. Roeder, O. Lenchuk, D. Mollenhauer, P. Adelhelm, *Adv. Energy Mater.* **2018**, *8*, 1702724.
- [23] A. Lago, M. A. Rivas, J. Legido, T. P. Iglesias, *J. Chem. Thermodyn.* **2009**, *41*, 257.
- [24] L. Simeral, R. L. Amey, *J. Phys. Chem.* **1970**, *74*, 1443.
- [25] R. H. Beaumont, B. Clegg, G. Gee, J. Herbert, D. J. Marks, R. C. Roberts, D. Sims, *Polymer* **1966**, *7*, 401.

- [26] H. Fujimori, M. Oguni, *J. Chem. Thermodyn.* **1994**, *26*, 367.
- [27] M. Tanwar, H. K. Bezabh, S. Basu, W.-N. Su, B.-J. Hwang, *ACS Appl. Mater. Interfaces* **2019**, *11*, 39746.
- [28] A. C. S. Jensen, H. Au, S. Gärtner, M.-M. Titirici, A. J. Drew, *Batteries Supercaps* **2020**, *3*, 1306.
- [29] G. Kamath, R. W. Cutler, S. A. Deshmukh, M. Shakourian-Fard, R. Parrish, J. Huether, D. P. Butt, H. Xiong, S. K. R. S. Sankaranarayanan, *J. Phys. Chem. C* **2014**, *118*, 13406.
- [30] Q. Liu, F. Wu, D. Mu, B. Wu, *Phys. Chem. Chem. Phys.* **2020**, *22*, 2164.
- [31] M. Shakourian-Fard, G. Kamath, K. Smith, H. Xiong, S. K. R. S. Sankaranarayanan, *J. Phys. Chem. C* **2015**, *119*, 22747.

Manuscript received: January 25, 2023

Accepted manuscript online: March 16, 2023

Version of record online: April 19, 2023